JOURNAL OF
Materials
CHEMISTRY

Supramolecular fullerene chemistry: synthesis, crystal structure and potassium intercalation of $[(C_{60})][(C_6H_5)_2]$

Alain Pénicaud,*[a] Olinda Y. Carreón,[a] Aurélie Perrier,[a] David J. Watkin[b] and Claude Coulon[a]

[a]*Centre de Recherche Paul Pascal, UPR 8641 CNRS, Université de Bordeaux-I, Av. Schweitzer, 33600 Pessac, France. E-mail: penicaud@crpp.u-bordeaux.fr*
[b]*Chemical Crystallography Laboratory, Oxford University, 9 Parks Road, Oxford, UK OX1 3PD*

Received 23rd July 2001, Accepted 3rd December 2001
First published as an Advance Article on the web 12th February 2002

Cocrystallization of C_{60} and biphenyl affords neutral mixed single crystals, which present close compact arrays of C_{60} molecules and vacant sites. Intercalation with potassium at low temperature (80 °C) affords a new, ternary, fulleride salt. Additionally, a simple model has been developed to describe the kinetics of intercalation.

It is strongly felt that breakthroughs in fullerene based materials will come from solid state chemistry through increased complexity.[1,2] After the early successes of (exohedral) alkali metal doping of C_{60}, several attempts have been made to generate new salts. Varied stoichiometries in mixtures of the doping metal led to a wealth of materials, such as the superconducting A_3C_{60} phases[3] and the polymeric A_1C_{60} compounds,[4] which have recently been reviewed;[1] ternary crystals containing C_{60}, NH_3 and an alkali metal have been obtained.[1] Other attempts were made with organic or organometallic cations, which have recently been reviewed,[5] the most notable result being the synthesis of the ferromagnetic TDAE·C_{60}.[6] In the meantime, extended effort has been devoted to the supramolecular chemistry of C_{60}.[7–10] In particular, a number of neutral mixed crystals (containing a fullerene and another neutral constituent) have been reported in the literature. For example, C_{60} crystallizes with iodine to give a neutral mixed crystal of formula $C_{60}I_4$, with $d_{\text{center-to-center}}$ (d_{ctc}) values of 9.96 and 9.98 Å.[11] Other early examples of such neutral fullerene containing compounds were obtained by cocrystallizing C_{60} with a U-shaped bis-BEDT-TTF molecule, ferrocene, BEDT-TTF, benzene, iodine, phosphorous, sulfur and twinTDAS to afford the corresponding mixed crystals (bis-BEDT-TTF)C_{60},[12] C_{60}(ferrocene)$_2$,[13] (BEDT-TTF)$_2C_{60}$,[14] $C_{60}(C_6H_6)_4$,[15] $C_{60}I_2$(toluene),[16] $C_{60}(P_4)_2$,[17] $C_{60}(S_8)_2$,[18] and $(C_{60})_4$(twinTDAS)$_3$.[19] In all of these mixed crystals, the closest d_{ctc} values range from 9.90 to 10.64 Å, values comparable to the d_{ctc} in neutral C_{60} or in K_3C_{60}. Of course these materials, having no unpaired electrons, do not exhibit magnetic phenomena nor electrical conductivity. But they are still important in the sense that they tell us that structures with C_{60} molecules in contact *can be made* out of the alkali metal field. This is actually of renewed interest since the report by Batlogg *et al.* of field induced superconductivity below 50 K in pristine (neutral) C_{60}.[20] We report here on the synthesis of a novel neutral mixed fullerene compound with biphenyl as a guest and its subsequent intercalation with potassium. To the best of our knowledge, there is only one previously reported case of a neutral mixed crystal of C_{60} being subsequently doped.[21]

Experimental

X-Ray analysis on single crystals of the neutral compound were performed on a CAD4 diffractometer (NONIUS) at room temperature and on an imaging plate system (STOE IPDS) at 155 K. Thermal analysis was performed on a Perkin Elmer PYRIS differential scanning calorimeter. Intercalation of the neutral compound with K was done in sealed ESR tubes with one end containing the neutral binary compound C_{60} biphenyl and the other end containing the alkali metal. Experiments were performed at 80 °C. The tubes were periodically checked by ESR to follow the kinetics of intercalation. The ESR spectra were obtained with a Bruker ESP 300E spectrometer equipped with an Oxford Instruments Helium Cryostat.

Results and discussion

A. The neutral compound $[(C_{60})][(C_6H_5)_2]$

Slow cocrystallization of saturated solutions of C_{60} and biphenyl in toluene at ambient temperature afforded black shiny single crystals of the neutral mixed compound of formula $[(C_{60})][(C_6H_5)_2]$ after four weeks. Fast cocrystallization yielded bulk quantities of the same materials as a microcrystalline powder.[22] X-Ray analysis was performed on a single crystal at room temperature and 155 K.[23] In both cases, the structure is monoclinic, with the *c* axis doubled at low temperature. A view of the room temperature unit-cell is represented in Fig. 1. C_{60} and biphenyl molecules are located at 2/*m* positions at (0, 1/2, 0) and (0, 0, 1/2) respectively. The structure is best conceptualized as comprised of alternating fullerene and biphenyl planes along the *c* axis. Within a C_{60} plane, the unit pattern is a rhombus of side 9.942 Å and of diagonals 10.424 and 16.932 Å. Tiling of the plane with these rhombs leads to a pseudo-hexagonal 2D network with parameters 9.942 and 10.424 Å and an angle of 121.6°. These planes repeat each other along the *c* axis, resulting in an AAA pseudo hexagonal C_{60} network. Such a packing has already been reported for $NMe_4^+C_{60}^-$ [24] The biphenyl planes are identical but shifted so that the apex of a rhombus faces the center of a rhombus of the neighboring plane. In terms of molecular packing, this leads to a polyhedral shape where the apices are occupied by one component and the center by the other one. This shape is in fact a cube that has been elongated along a (110) diagonal. This structure is thus remotely related to the CsCl structure. Hence, each molecular component A (C_{60} or biphenyl) has eight B neighbors. C_{60}, being the close packed constituent, has eight C_{60} neighbors: six in the (*a*,*b*) pseudohexagonal plane and two along the *c* axis at −1 and +1. So, each C_{60} has 4 neighboring C_{60}'s at 9.942 Å (sides of the rhombs), 2 at 10.424 Å (short diagonal of the rhomb) and 2 at 10.320 Å (along *c*) to be compared with 10.0 Å

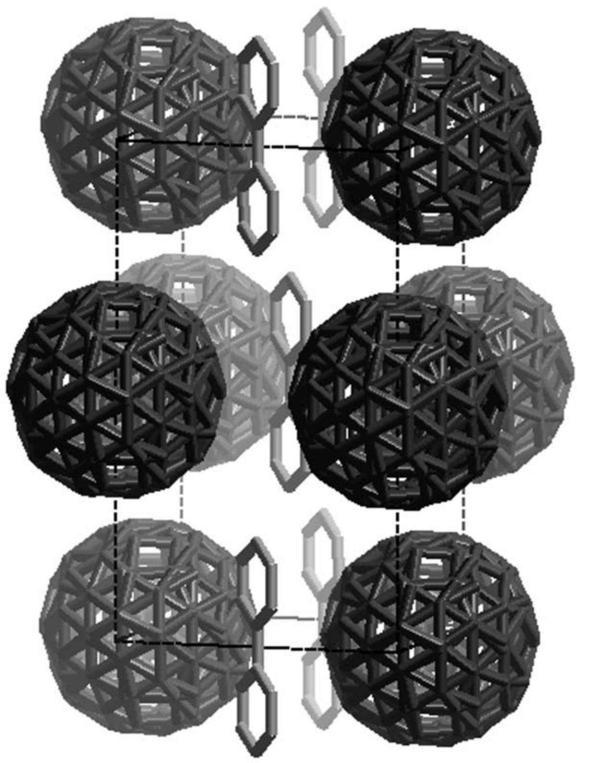

Fig. 1 Projection of the unit-cell of [(C_{60})][($C_6H_5)_2$] at 293 K; *b* axis is vertical, *c* axis is horizontal; hydrogen atoms have been omitted for clarity.

in pristine C_{60}. Thus, the prerequisite of close contacts between C_{60}'s for cooperative properties is fulfilled in this structure.

At room temperature, the C_{60} molecules are disordered (two orientations with 50% occupancy factor were refined, Fig. 2a) whereas a planar conformation was observed for the biphenyl (Fig. 2c). At 155 K, the C_{60}'s are now ordered (Fig. 2b) with one orientation per site and the resulting unit-cell is doubled along the *c*-axis (Fig. 3). The packing is identical, the rhombs now having sides of 9.926 Å and a short diagonal of 10.399 Å, the out of plane contact along *c* now being 10.232 Å. These correspond to respective shrinkages of 0.16, 0.24 and 0.85%. Thus, compacity is mostly increased between the fullerene planes rather than within the planes. At 155 K, the biphenyl molecules have adopted a twisted conformation (Fig. 2d) with a torsion angle between the two phenyl planes of 22.9° to be compared with 10° in pristine biphenyl at low temperature.[25] Further studies by X-ray diffuse scattering as a function of temperature are under way to study the phase(s) transition(s) of [(C_{60})][($C_6H_5)_2$].[26]

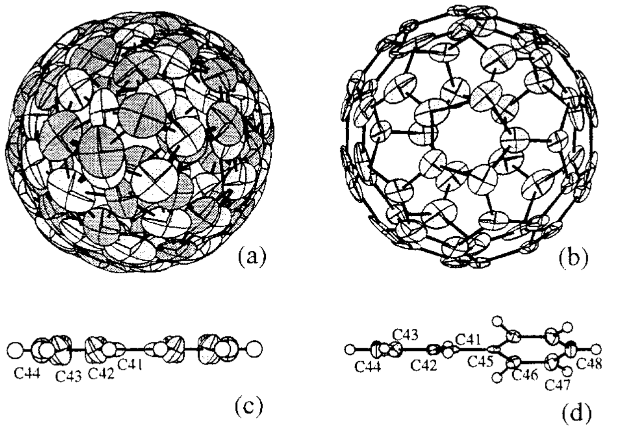

Fig. 2 C_{60} and biphenyl at room temperature (a and c) and 155 K (b and d).

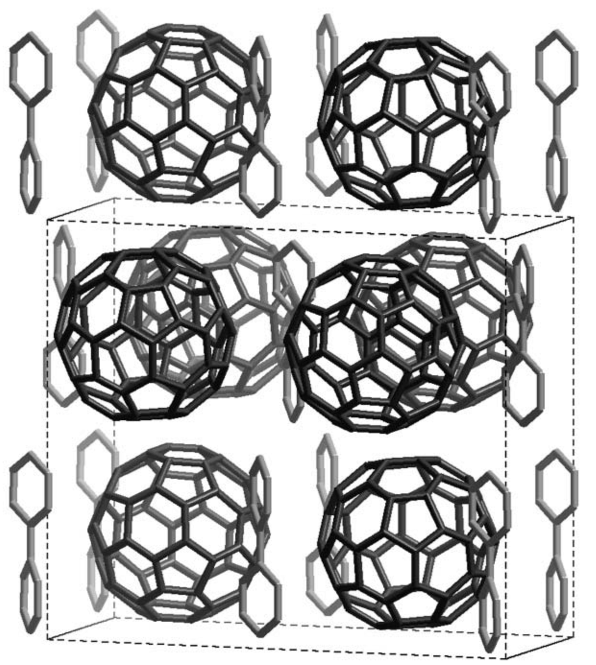

Fig. 3 Projection of the unit-cell of [(C_{60})][($C_6H_5)_2$] at 155 K; *b* axis is vertical, *c* axis is horizontal; hydrogen atoms have been omitted for clarity.

In order to assess the feasibility of alkali metal intercalation, identification of potential doping sites was undertaken. The C_{60}'s form a pseudo-hexagonal plane, there might be empty sites bordered by a triangle of C_{60}'s. There are 8 such sites per unit-cell (for 2 C_{60}'s and 2 biphenyl), hence maximum doping with conservation of the molecular architecture should lead to the formula M_4[(C_{60})][($C_6H_5)_2$]. Outside the plane, these sites are cornered by a biphenyl hydrogen atom, namely H(431) (Fig. 4). Taking into consideration van der Waals radii of 1.2 Å and 5 Å for hydrogen and C_{60} respectively, one finds a tetrahedral site of 1.1 Å radius comparable to the empty sites of pristine C_{60}.[27]

Thermal analysis was performed on [(C_{60})][($C_6H_5)_2$] and on biphenyl as a comparison. Melting of pure biphenyl, occurring at 71.3 °C, is no longer observable for [(C_{60})][($C_6H_5)_2$]; for both compounds, degradation started to occur around 140 °C.

B. Intercalation with potassium

For preliminary experiments, potassium was chosen as a compromise between size and reasonable vapour pressure at

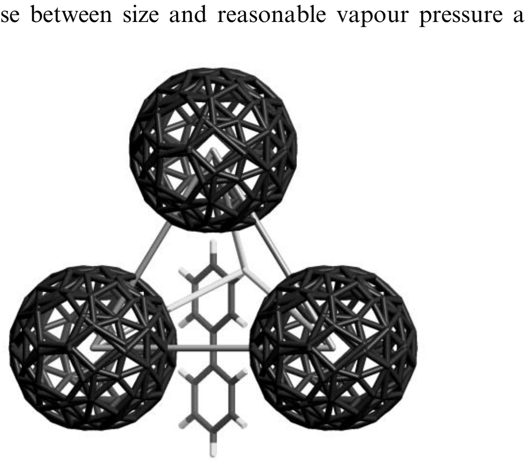

Fig. 4 Available vacant site for intercalation (at room temperature).

such low temperatures. Doping was attempted in the following way: excess potassium was loaded into a reservoir at the end of an ESR tube containing *ca.* 1 mg of $[(C_{60})][(C_6H_5)_2]$; the ESR tube was then taken outside the glove box, sealed under vacuum and placed in an oven with the $[(C_{60})][(C_6H_5)_2]$ zone at 80 °C and the potassium end at 76 °C; the tube was periodically removed from the oven and its ESR spectrum measured as a function of time. At the end of the experiment, the tube was opened to air to check the air sensitivity of the phases formed.

Evolution with time

Time dependent ESR spectra show a composite signal whose intensity rises with heating time. This signal can be deconvoluted with a model of two Lorentzian lines (inset of Fig. 5) albeit their *g*-values cannot be separated since their resonance field is very similar. The *g*-value for the global signal is 2.0006 and stays constant with time (up to 400 hours). The linewidths of the two signals are 3.5 Gauss (signal A) and 14 Gauss (signal B). The ESR intensity as a function of time is plotted in Fig. 5. For both signals, there is a slow rising at short times followed by a faster increase of the intensity with an inflexion point and finally, the intensity saturates at longer times.

Temperature dependence

Measurements as a function of temperature were performed near the inflexion point and at the beginning of the plateau. Measurements at longer times were not performed since the tube was opened to check the air sensitivity of the compounds formed. In fact, the two experiments yielded qualitatively the same results, and we shall describe them together. The *g*-values could not be resolved down to 40 K, the temperature below which the *g*-value for signal A rises to reach 2.0010 at helium temperature whereas the *g*-value for signal B diminishes to reach 1.9998 at 4 K. Additionally, below 19 K, a zero field absorption is observed, revealing the presence of a superconducting phase.[28] The linewidth of the B signal and its temperature dependence are similar to that reported for early experiments of potassium intercalation of pristine C_{60}.[29] Thus, it was concluded that signal B (the major phase) corresponds to a binary K_xC_{60} phase,[30] whereas signal A corresponds to a new, ternary phase $K_n[(C_{60})][(C_6H_5)_2]$.[34] It should be noted that, at helium temperature, an extra signal can be detected with a high *g*-value (2.0040). This signal has been already reported to correspond to a high doped stage of K_xC_{60}.[28] The tube was then opened at room temperature to test the air sensitivity of phase A. As expected, the signal corresponding to B and the extra signal at $g = 2.0040$ are lost in less than a day. Interestingly enough, signal A does not disappear upon exposure to air, at least for a few days.[36]

A new temperature study revealed that the remaining signal A is pure. The *g*-value is constant (2.0006) from room temperature down to 30 K where it rises to reach 2.0011 at 4 K (Fig. 6b). The signal intensity and linewidth *vs.* temperature are plotted in Figs. 6a and 6c respectively. The spin susceptibility rises slightly when lowering the temperature. This behaviour may be indicative of a conducting character for the compound studied. Below 25 K, it begins to decrease which could indicate a transition towards an antiferromagnetic state with T_N of the order of 4 K.[37] Further work is in progress to characterize this new fulleride salt.

Kinetics analysis

There are previous reports of a kinetic analysis of the intercalation of alkali metal into pristine C_{60}. The Avrami model is usually considered to fit the experimental data, as for example in the work of Stankowski *et al.*[38]

Originally, the Avrami model, developed in the 40's, described the transformation of one phase into another during the kinetics of a first order phase transition. The principal assumptions of this model are the following. It is assumed that nucleation centers are already present at the beginning of the kinetics, with a density $\bar{N}$. During the kinetics, the nucleation centers become activated to generate domains of the new phase, with a characteristic time τ_1. If this process would

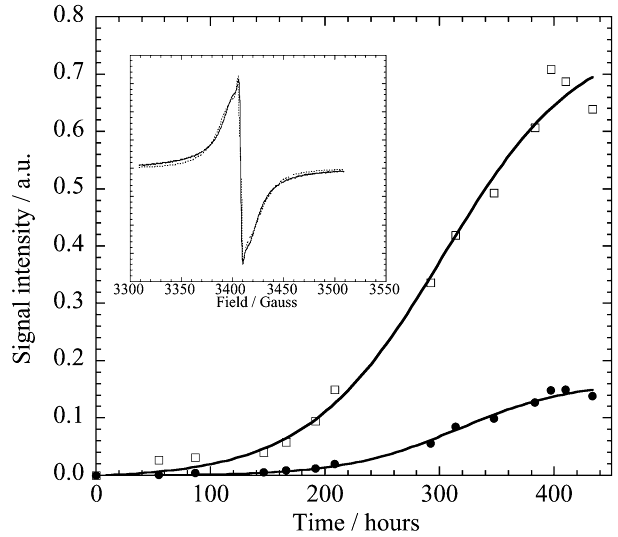

Fig. 5 ESR intensity *vs.* heating time for signals A (full symbols) and B (open symbols). solid lines are fitted to the model discussed later in the text. Inset: deconvolution of the ESR spectra of $[(C_{60})][(C_6H_5)_2]$ + K with two Lorentzian derivatives. Solid line: experimental, dashed line: fit.

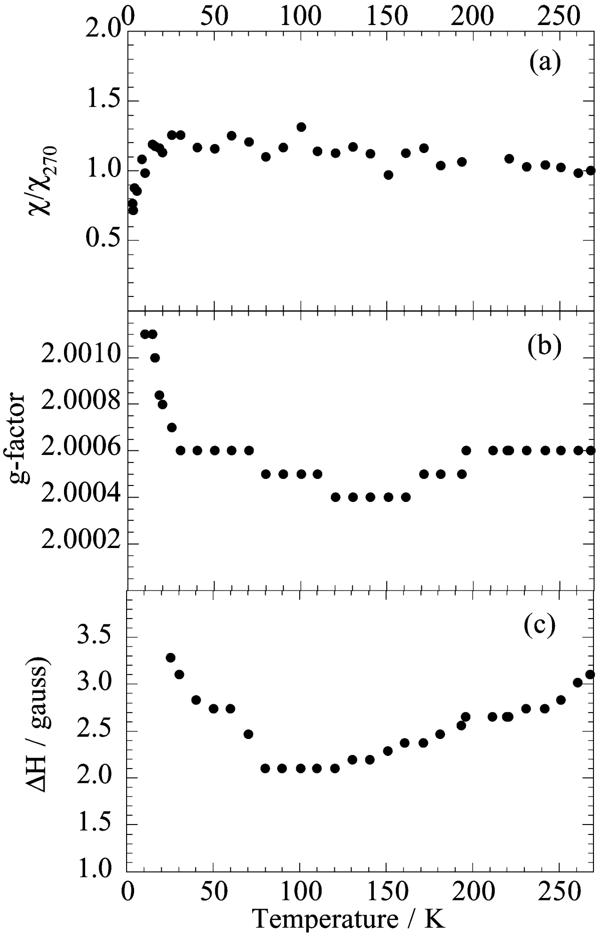

Fig. 6 (a) Normalized spin susceptibility *vs.* temperature for $K_n[(C_{60})][(C_6H_5)_2]$. (b) *g*-value *vs.* temperature; (c) Linewidth *vs.* temperature.

be the only one to be considered, the density of activated centers at time t would be $\bar{N}\,(1-e^{-t/\tau_1})$. In fact, at a given time, the activation of new nucleation centers competes with the growth of already existing domains of the new phase. The linear size of these domains is assumed to vary linearly with time, with a characteristic time τ_2 *i.e.* $R(t) \propto \frac{t-t_0}{\tau_2}$ for a domain activated at the time t_0. Therefore the volume of this domain scales like $\left(\frac{t-t_0}{\tau_2}\right)^3$ in three dimensions. The description of the resulting kinetics is rather complicated in the general case.[39] However, a simplified version of the model exists assuming a random distribution of the nucleation centers. In this case,[40] the volume fraction, $x(t)$, of the new phase reads: $x(t) = 1-e^{-V_{ext}(t/\tau_1)}$, with:

$$V_{ext}(\tau) = \frac{8\pi\bar{N}\tau_1^3}{\tau_2^3}E(\tau), \text{ where } \tau = t/\tau_1$$

and:

$$E(\tau) = e^{-\tau} - 1 + \tau - \frac{\tau^2}{2} + \frac{\tau^3}{6}.$$

When the condition $\frac{\bar{N}\tau_1^3}{\tau_2^3} \ll 1$ is satisfied, the expression of $x(t)$ can be approximated to:

$$x(t) = 1 - e^{-(4\pi\bar{N}t^3)/(3\tau_2^3)}$$

i.e. $x(t)$ becomes independent of the characteristic time τ_1.

It is this latter simplified expression which is used in reference 38 to describe the kinetics of intercalation in C_{60}. In this paper, a slightly better fit is obtained using an empirical generalisation of the Avrami model, called the "Johnson–Mehl–Avrami" model, where $x(t)$ reads:

$$x(t) = 1 - e^{-Kt^n}$$

In this model, the exponent n becomes a new adjustable parameter. As the $n = 3$ value found in the original approximate expression of $x(t)$ comes from the assumption of growth of 3D compact domains, one may assume that values of the exponent n smaller than 3 are indicative of a lower dimensional process, for example nucleation favoured at the surface of the material. However, this analysis remains highly empirical as the general expression deduced from the Avrami model is much more complicated when the assumption of randomness of distribution of the nucleation centres is released. Moreover, using the above expression of $x(t)$, the parameters $\bar{N}$ and τ_2 cannot be determined independently (they both enter in the expression of the parameter K) and the relevance of the model cannot be easily discussed.

Another important question arises when using the Avrami model to describe an intercalation process. In the kinetics of a first order phase transition, the assumption of compact domains of the new phase which is consistent with the scaling law $R(t) \propto \frac{t-t_0}{\tau_2}$ directly arises from the existence of a large interfacial tension between the two phases. As a consequence, the shape of the aggregates is chosen to minimize the surface between the two phases. On the other hand, in the intercalation process, one may imagine different shapes of these domains resulting from a different assumption. A limiting case will be obtained assuming negligible effect of the interfacial energy between undoped and doped domains. In this latter case, we show below that we can obtain a different expression of $x(t)$ to fit the experimental data.

Let us develop a simple kinetic model to determine $x(t)$, the fraction of doped sites at the time t (we shall call a site an elementary volume of the material, for example a unit-cell, without the need to further define it). We shall introduce two characteristic times τ_1 and τ_2 to describe the doping process of undoped (empty) sites. The first one is the characteristic time to dope an empty site surrounded by empty sites (*i.e.* to activate a new domain of the doped phase). Similarly, the doping of an empty site adjacent to an already doped site will be described by the characteristic time τ_2 which therefore describes the growth of the doped domains. A physically reasonable assumption is $\tau_1 \gg \tau_2$ as it is certainly easier to introduce an alkali atom in the surrounding of a doped site where the lattice already has the characteristics of the new phase. No other assumption will be made to further discriminate the different sites during the doping process. As the probability of finding an empty site close to an empty or a doped site respectively reads $(1-x)^2$ and $x(1-x)$ (the sum of these two probabilities is $1-x$, the probability of finding an empty site at the time t), the evolution of $x(t)$ with time is given by:

$$\frac{dx}{dt} = \frac{(1-x)^2}{\tau_1} + \frac{x(1-x)}{\tau_2}$$

Note that this equation is the generalisation (when $\tau_1 \neq \tau_2$) of the well known expression which describes first order kinetics, *i.e.* $\frac{dx}{dt} = \frac{1-x}{\tau}$.

An exact solution can be obtained and reads:

$$x(t) = \frac{e^{t/\tau_2} - 1}{e^{t/\tau_2} + \frac{\tau_1}{\tau_2} - 1}$$

The inset of Fig. 7 shows the resulting shape of $x(t)$ as a function of t/τ_2, for different values of the reduced parameter $\gamma = \frac{\tau_1}{\tau_2} - 1$. An inflexion point is found for $\gamma > 1$ (*i.e.* $\tau_1 > 2\tau_2$), such as $t_{\text{Inf}} = \tau_2 \ln\gamma$. For smaller values of γ, the shape is qualitatively the same as for simple first order kinetics (corresponding to $\gamma = 0$) as the slope of the curve continuously decreases with time. Note that the initial slope becomes infinite as γ approaches -1 ((*i.e.* for $\tau_1 \ll \tau_2$).

The relation with the experimental data is straightforward assuming that empty sites are diamagnetic whereas doped sites are paramagnetic. The intensity of the ESR signal is thus proportional to $x(t)$. Following our model, the "S shape" curve obtained experimentally (see Fig. 5) shows that we are in the case where $\tau_1 > 2\tau_2$, in agreement with the arguments given to introduce this model. Note that a similar conclusion does not apply to the Avrami model for which an inflexion point is always found. To preserve the assumption $\tau_1 \gg \tau_2$ together with the condition of validity of the simplified model, $\frac{\bar{N}\tau_1^3}{\tau_2^3} \ll 1$, it is necessary to assume $\bar{N} \ll 1$, *i.e.* that the density of nucleation

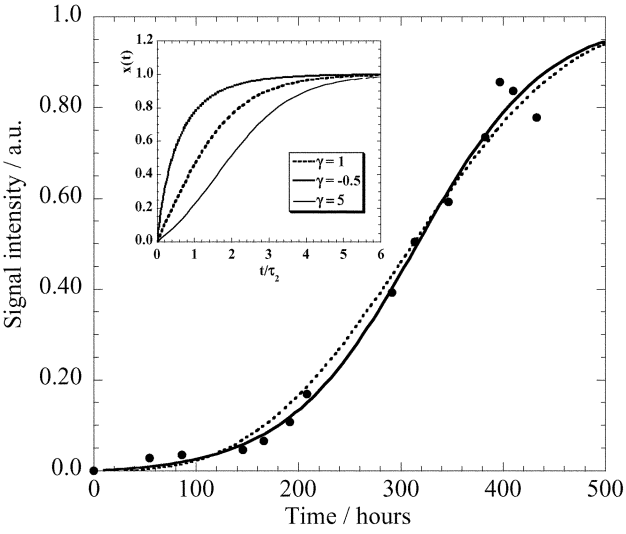

Fig. 7 Total ESR intensity *vs.* time. The dotted line is a fit by Avrami's model,[40] the full line is a fit by the model described in this report (see text). Inset: fraction of doped sites as a function of t/τ_2 for different values of $\gamma = \tau_1/\tau_2 - 1$, as deduced from the kinetic model developed in the text.

centers is very small, which is unlikely in the case of intercalation. For this reason and because the assumption of spherical growth of the intercalated domains is rather artificial, we believe that the model developed in this report is relevant to describe intercalation processes.

Let us now discuss our experimental data. As already mentioned, during the potassium intercalation of $[(C_{60})][(C_6H_5)_2]$, we have observed the appearance of two distinct doped phases, namely K_xC_{60} and $K_n[(C_{60})][(C_6H_5)_2]$. Their kinetics, though, are very similar, as exemplified in Fig. 5 and by the fact that the two temperature dependent experiments, performed after 292 and 411 hours gave the same proportion of each. So, for the purpose of kinetics analysis, it is possible to regard this doping process as the doping of a single phase. Although the experimental data could be fitted using the simplified version of the Avrami model (see Fig. 7), we shall use our model which also gives a satisfactory fit (continuous line in Fig. 7). We obtain the following parameters: $\tau_2 = 63 \pm 4$ h and $\tau_1 = 9200 \pm 2600$ h. Hence, for both phases, τ_1 is much larger than τ_2, exemplifying the fact that growth is far easier than nucleation.

Conclusion

The crystal structure of $[(C_{60})][(C_6H_5)_2]$ exhibits an extended network of C_{60} molecules in contact with empty sites of adequate size for insertion of metallic cations. Intercalation with potassium affords a new, ternary, fulleride salt. The kinetics of intercalation can be fitted with a simple model yielding two characteristic time scales.

It is our conviction that the example described in this report opens a novel synthetic route towards fulleride salts. In particular, there are already a large number of neutral mixed C_{60} compounds, several of which could certainly be intercalated with alkali metals and, furthermore, such neutral networks are not limited by the periodic table, contrary to the intercalated species, and possibilities are, thus, infinite. The strategy we propose can be outlined as follows: (i) synthesis of neutral mixed crystals of fullerenes and molecular partners; (ii) identification of close compact 1D, 2D or 3D fullerene networks and of empty sites suitable to be filled up; (iii) intercalation of those sites akin to the doping of pristine C_{60}. Indeed, the close compact condition is necessary if one is looking for cooperative electronic properties such as (super)-conductivity and (anti)ferromagnetism. The molecular counterpart of C_{60} offers variety (in the architectures formed) but also a way to fine-tune the topologies of the networks obtained, using the general strategy of modern crystal engineering.[41] Random searching of molecular partners has already led to a number of interesting structures.[42] With increasing knowledge of the rationales behind packing in those architectures, one should be able to play some modest crystal structure engineering and obtain tailor made neutral mixed crystals, suitable for subsequent metal intercalation. Additionally, the synthesis of novel mixed neutral networks of C_{60} and the accompanying screening of the structures for extended networks of C_{60} molecules in contact, offer new candidates for potential field induced conductors or superconductors.[20]

Acknowledgement

We thank Professor G. Sigaud for the thermal analysis, Dr J. Darriet for use of the CAD4 diffractometer and Drs P. Batail and K. Boubekeur for the use of the IPDS system. AP thanks the Royal Society of Chemistry for a travel grant to visit DW, OC thanks CONACyT (Mexico) for a PhD. grant.

References

1 M. J. Rosseinsky, *Chem. Mater.*, 1998, **10**, 2665–2685.

2 A. Pénicaud, *Fullerene Sci. Technol.*, 1998, **6**, 731–741.

3 A. F. Hebard, M. J. Rosseinsky, R. C. Haddon, D. W. Murphy, S. H. Glarum, T. T. M. Palstra, A. P. Ramirez and A. R. Kortan, *Nature*, 1991, **350**, 600–601.

4 S. Pekker, A. Jánossy, L. Mihaly, O. Chauvet, M. Carrard and L. Forró, *Science*, 1994, **265**, 1077–1078.

5 C. A. Reed and R. D. Bolskar, *Chem. Rev.*, 2000, **100**, 1075–1119.

6 P. M. Allemand, K. Khemani, A. Koch, F. Wudl, K. Holczer, S. Donovan, G. Grüner and J. D. Thompson, *Science*, 1991, **253**, 301.

7 F. Diederich and M. Gómez-López, *Chem. Soc. Rev.*, 1999, **28**, 263–277.

8 A. Balch and M. M. Olmstead, *Coord. Chem. Rev.*, 1999, **185-186**, 601–617.

9 M. J. Hardie and C. L. Raston, *Chem. Commun.*, 1999, 1153–1163.

10 P. D. W. Boyd, M. C. Hodgson, C. E. F. Rickard, A. G. Oliver, L. Chaker, P. J. Brothers, R. D. Bolskar, F. S. Tham and C. A. Reed, *J. Am. Chem. Soc.*, 1999, **121**, 10487–10495; D. V. Konarev, I. S. Neretin, Y. L. Slovokhotov, E. I. Yudanova, N. V. Drichko, Y. M. Shul'ga, B. P. Tarasov, L. G. Tumanov, A. S. Batsanov, J. H. K. Howard and R. N. Lyubovskaya, *Chem. Eur. J.*, 2001, **7**, 2605–2616.

11 Q. Zhu, D. E. Cox, J. E. Fischer, K. Kniaz, A. R. McGhie and O. Zhou, *Nature*, 1992, **355**, 712.

12 I. Izuoka, T. Tachikawa, T. Sugawara, Y. Saito and H. Shinohara, *Chem. Lett.*, 1992, 1049–1052.

13 J. D. Crane, P. B. Hitchcock, H. W. Kroto, R. Taylor and D. R. M. Walton, *J. Chem. Soc., Chem. Commun.*, 1992, 1764–1765.

14 I. Izuoka, T. Tachikawa, T. Sugawara, Y. Suzuki, M. Konno, Y. Saito and H. Shinohara, *J. Chem. Soc., Chem. Commun.*, 1992, 1472–1473.

15 M. F. Meidine, P. B. Hitchcock, H. W. Kroto, R. Taylor and D. R. M. Walton, *J. Chem. Soc., Chem. Commun.*, 1992, 1534; A. L. Balch, J. W. Lee, B. C. Noll and M. M. Olmstead, *J. Chem. Soc., Chem. Commun.*, 1993, 56–58; H. B. Bürgi, R. Restori, D. Schwarzenbach, A. L. Balch, J. W. Lee, B. C. Noll and M. M. Olmstead, *Chem. Mater.*, 1994, **6**, 1325–1329.

16 A. G. Avent, P. R. Birkett, C. Christides, J. D. Crane, A. D. Darwish, P. B. Hitchcock, H. W. Kroto, M. F. Meidine, K. Prassides, R. Taylor and D. R. M. Walton, *J. Mol. Struct.*, 1994, **325**, 1–11.

17 I. Wyn Locke, A. D. Darwish, H. W. Kroto, K. Prassides, R. Taylor and D. R. M. Walton, *Chem. Phys. Lett.*, 1994, **225**, 186–190.

18 G. Roth and P. Adelmann, *Appl. Phys.*, 1993, **A56**, 169; O. A. Dyachenko, E. B. Yagubskii, S. V. Konovalikhin, N. D. Kushch, G. V. Shilov and N. G. Spitsina, *Mol. Mater.*, 1994, **4**, 133–135; L. I. Buravov, O. A. D'yachenko, S. V. Konovalikhin, N. D. Kushch, I. P. Lavrent'ev, N. G. Spitsina, G. V. Shilov and E. B. Yagubskii, *Russ. Chem. Bull.*, 1994, **43**, 240–244.

19 A. I. Kotov, S. V. Konovalikhin, R. V. Pisarev, G. V. Shilov, O. A. Dyachenko and E. B. Yagubskii, *Mendeleev Commun.*, 1994, 180–182; A. Pénicaud, K. Boubekeur, A. I. Kotov and E. B. Yagubskii, *Acta Crystallogr., Sect. B: Struct. Crystallogr. Cryst. Chem.*, 2000, **B56**, 497–500.

20 J. H. Schön, Ch. Kloc and B. Batlogg, *Nature*, 2000, **408**, 549–552.

21 A. Otsuka, G. Saito, T. Teramoto, Y. Sugita, T. Ban, A. A. Zakhidov and K. Yakushi, *Mol. Cryst. Liq. Cryst.*, 1996, **284**, 345–357; Z. V. Vardeny, A. Epstein, A. A. Zakhidov and K. Yakushi, *Synth. Met.*, 1997, **85**, 1459–1460.

22 Toluene solutions of C_{60} (500 mg, 0.69 mmol in 300 ml) and $(C_6H_5)_2$ (107 mg, 0.69 mmol in 2 ml) were mixed and stirred at room temperature for 20 min. Toluene was removed under vacuum at room temperature, yieding 533 mg of a brown microcrystalline powder (yield 88%) whose composition was checked by X-ray powder diffraction and chemical analysis (observed: C, 97.99; H, 1.24. Calc.: C, 98.85; H, 1.15%).

23 Crystal data: $C_{72}H_{10}$, $M = 874.88$, $T = 293$ K, CAD-4, monoclinic, space group $C2/m$, $a = 10.424(5)$, $b = 16.932(9)$, $c = 10.320(5)$ Å, $\beta = 100.8\,(1)°$, $V = 1789.3$ Å^3, $F(000) = 884$, $Z = 2$, $d_{\text{calc}} = 1.62$ g.cm^{-3}, μ(Mo-Kα) $= 0.93$ cm^{-1}, crystal $0.2 \times 0.16 \times 0.44$ mm^3, 285 parameters, 2228 unique reflections for $0 < \theta < 28$ °, $R = 0.042$ for 883 reflections with $I > 3\sigma(I)$, Rw $= 0.048$, $S = 1.36$, $\rho_{\max} = 0.23$ e Å^{-3}, $\rho_{\min} = -0.24$ e Å^{-3}. T = 155 K, STOE IPDS, monoclinic, space group $I2/a$, $a = 10.399(1)$, $b = 16.910(1)$, $c = 20.464(2)$ Å, $\beta = 100.87(1)°$, $V = 3534.0$ Å^3, $F(000)$

$= 1768$, $Z = 4$, $d_{calc} = 1.64$ g cm^{-3}, μ(Mo-Kα) $= 0.94$ cm^{-1}, crystal $0.40 \times 0.24 \times 0.12$ mm^3, 332 parameters, 4153 unique reflections for $1.9 < \theta < 28.15°$, $R = 0.082$ for 1923 reflections with $I > 3\sigma(I)$, Rw $= 0.071$, $S = 1.16$, $\rho_{max} = 1.10$ e Å^{-3}, $\rho_{min} = -0.38$ e Å^{-3}. Both structures were refined with the CRYSTALS package[43] and Fig. 2 drawn with Ortep-3 for Windows.[44] For the low-temperature data, the solution was found using SIR92[45] and refined without restraints but on one C_{60} carbon atom whose *uij*'s were restrained. For the room-temperature data, atomic positions from the data at 155 K were input into the unit-cell at 293 K and their symmetrical counterpart generated. Then the structure was refined with restraints on the bond distances, similar *uij*'s for neighbouring atoms, and cycles planarity for the C_{60} molecule. A final refinement including all data (1380 reflections) was attempted but did not lead to a better result (by comparing the refined parameter values to the "theoretical" restrained ones)CCDC 170506 and 170507. See http://www.rsc.org/suppdata/jm/b1/b106580g/ for crystallographic files in .cif or other electronic format.

24 R. E. Douthwaite, M. A. Green, M. L. H. Green and M. J. Rosseinsky, *J. Mater. Chem.*, 1996, **6**, 1913–1920.

25 H. Cailleau, J. L. Baudour and C. M. E. Zeyen, *Acta Crystallogr., Sect. B: Struct. Crystallogr. Cryst. Chem.*, **35**, 426.

26 A. Marucci, P. Launois, R. Moret and A. Pénicaud, *Eur. Phys. J. B*, 2002, in the press.

27 M. S. Dresselhaus, G. Dresselhaus and P. C. Eklund, *Science of fullerenes and carbon nanotubes*, Academic Press, San Diego, 1996.

28 A. A. Zakhidov, A. Ugawa, K. Imaeda, K. Yakushi, H. Inokuchi, K. Kikuchi, I. Ikemoto, S. Suzuki and Y. Achiba, *Solid State Commun.*, 1991, **79**, 939–946.

29 J. Stankowski, P. Byszewski, W. Kempínski, Z. Trybula and T. Zuk, *Phys. Status Solidi B*, 1993, **178**, 221–231.

30 Although this K_xC_{60} phase was assigned in ref. 29 to K_3C_{60}, later work by three independent teams on stoichiometric K_3C_{60} (checked by X-ray diffraction) yielded different linewidths and temperature dependence[31–33].

31 K. Tanigaki, M. Kosaka, T. Manako, Y. Kubo, I. Hirosawa, K. Uchida and K. Prassides, *Chem. Phys. Lett.*, 1995, **240**, 627–632.

32 P. Petit, J. Robert, T. Yildirim and J. E. Fischer, *Phys. Rev. B*, 1996, **54**, R3764–R3767.

33 N. M. Nemes, J. E. Fischer, G. Baumgartner, L. Forró, T. Fehér, G. Oszlányi, F. Simon and A. Jánossy, *Phys. Rev. B*, 2000, **61**, 7118–7121.

34 The only known air stable binary K_xC_{60} phase is K_1C_{60} which forms by cooling down from high temperatures (above 150 °C) and has a larger linewidth: 4.5 G at 25 K, slowly increasing to 6.6 G at 300 K[35].

35 F. Bommeli, L. Degiorgi, P. Wachter, Ö. Legeza, A. Jánossy, G. Oszlanyi, O. Chauvet and L. Forro, *Phys. Rev. B*, 1995, **51**, 14794–14797.

36 After the measurement was done, the sample was kept under inert atmosphere as a precaution.

37 C. Coulon, J. C. Scott and R. Laversanne, *Phys. Rev. B*, 1986, **33**, 6235.

38 J. Stankowski, L. Kevan, B. Czyzak and B. Andrzejewski, *J. Phys. Chem.*, 1993, **97**, 10430–10432.

39 M. Avrami, *J. Chem. Phys.*, 1939, **7**, 1103.

40 M. Avrami, *J. Chem. Phys.*, 1940, **8**, 212.

41 *Cryst. Eng.*, 1998, **1** (whole issue).

42 References quoted in 2; D. V. Konarev, Y. V. Zubavichus, Y. L. Slovokhotov, Y. M. Shul'ga, V. N. Semkin, N. V. Drichko and R. N. Lyubovskaya, *Synth. Met.*, 1998, **92**, 1–6 and references therein.

43 CRYSTALS (issue 10): D. J. Watkin, C. K. Prout, J. R. Carruthers and P. W. Betteridge, 1996, Chemical Crystallography Laboratory, University of Oxford, Oxford; RC93: D. J. Watkin, C. K. Prout and P. M.deQ. Lilley (1994), Chemical Crystallography Laboratory, Oxford, UK; CAMERON: D. J. Watkin, C. K. Prout and L. J. Pearce (1996), Chemical Crystallography Laboratory, Oxford, UK.

44 L. J. Farrugia, *J. Appl. Cryst.*, 1997, 565.

45 A. Altomare, G. Cascarano, G. Giacovazzo, A. Guagliardi, M. C. Burla, G. Polidori and M. Camalli, *J. Appl. Cryst.*, 1994, **27**, 435'.